

Supplementary Figures

Figure S1

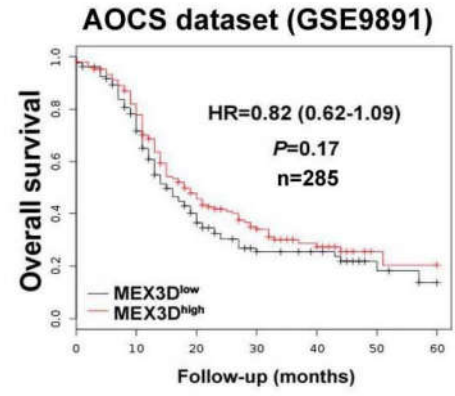
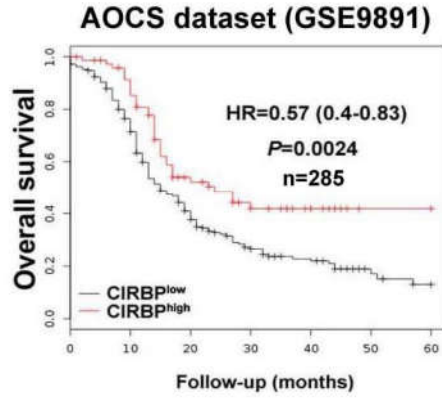
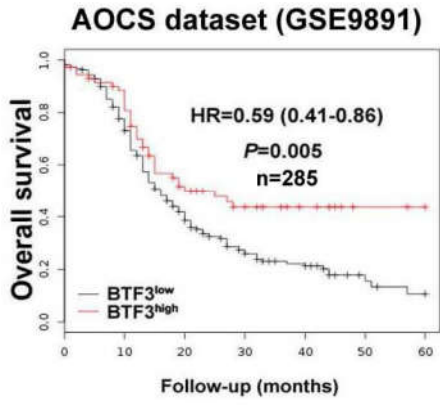
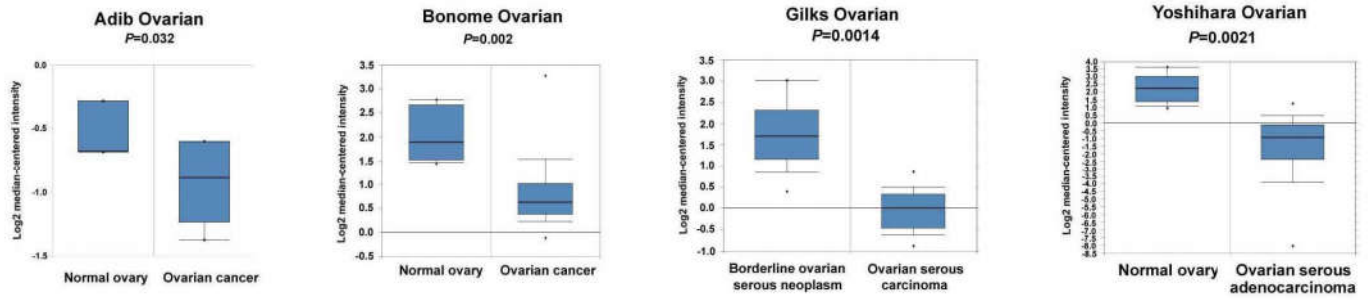
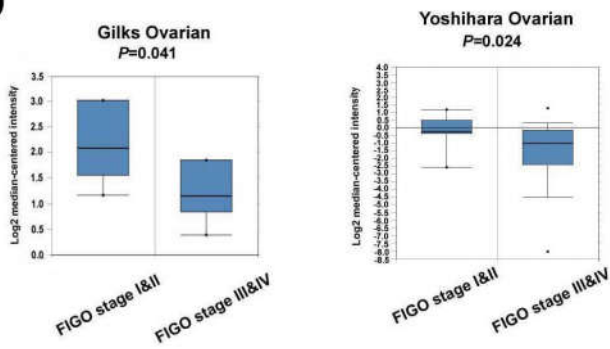


Figure S2

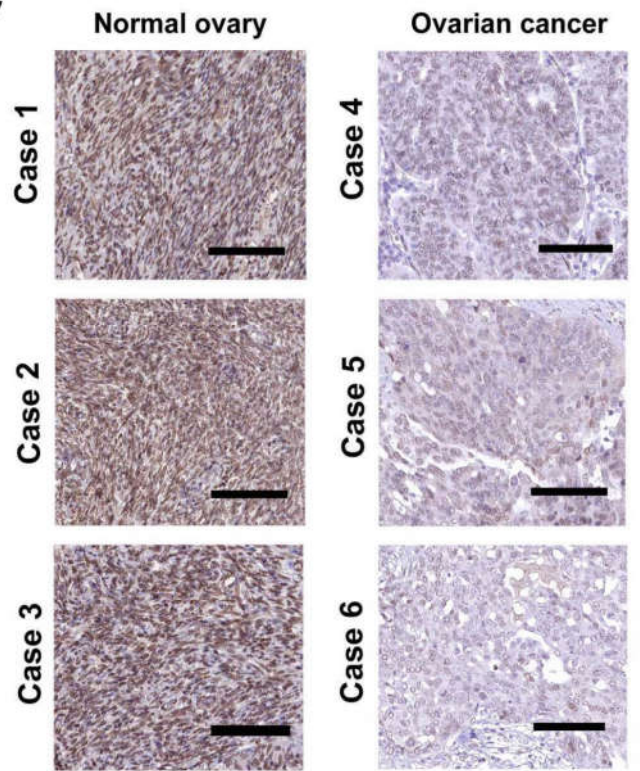
**a**



**b**



**c**



**d**

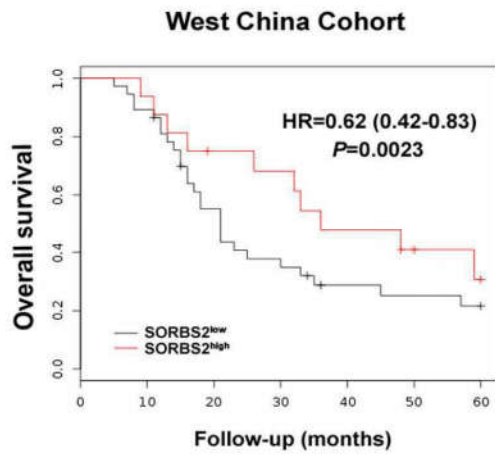
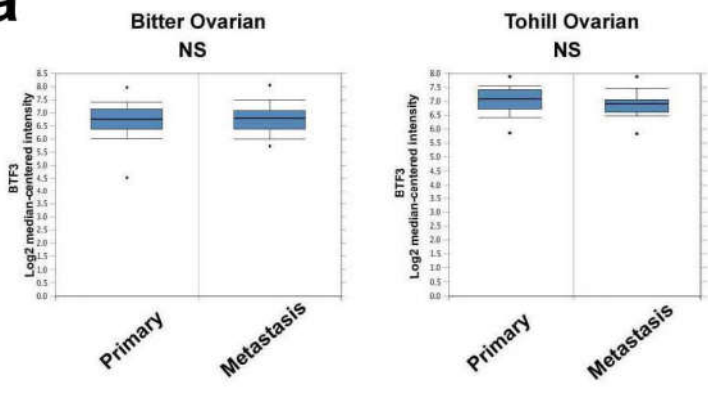
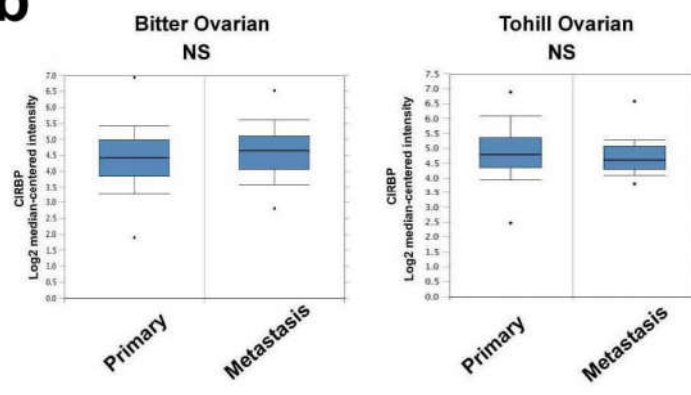


Figure S3

**a**



**b**



**c**

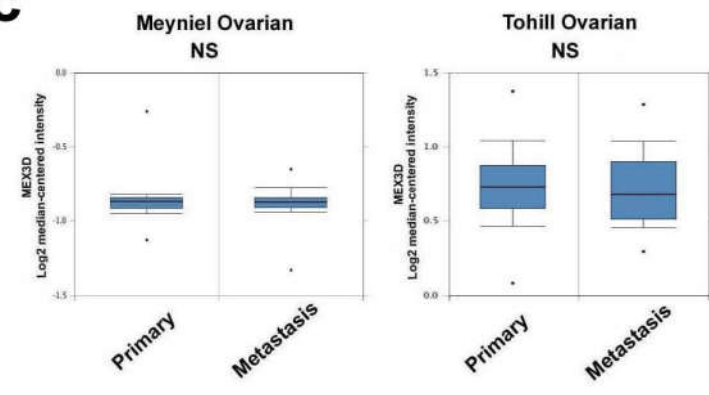


Figure S4

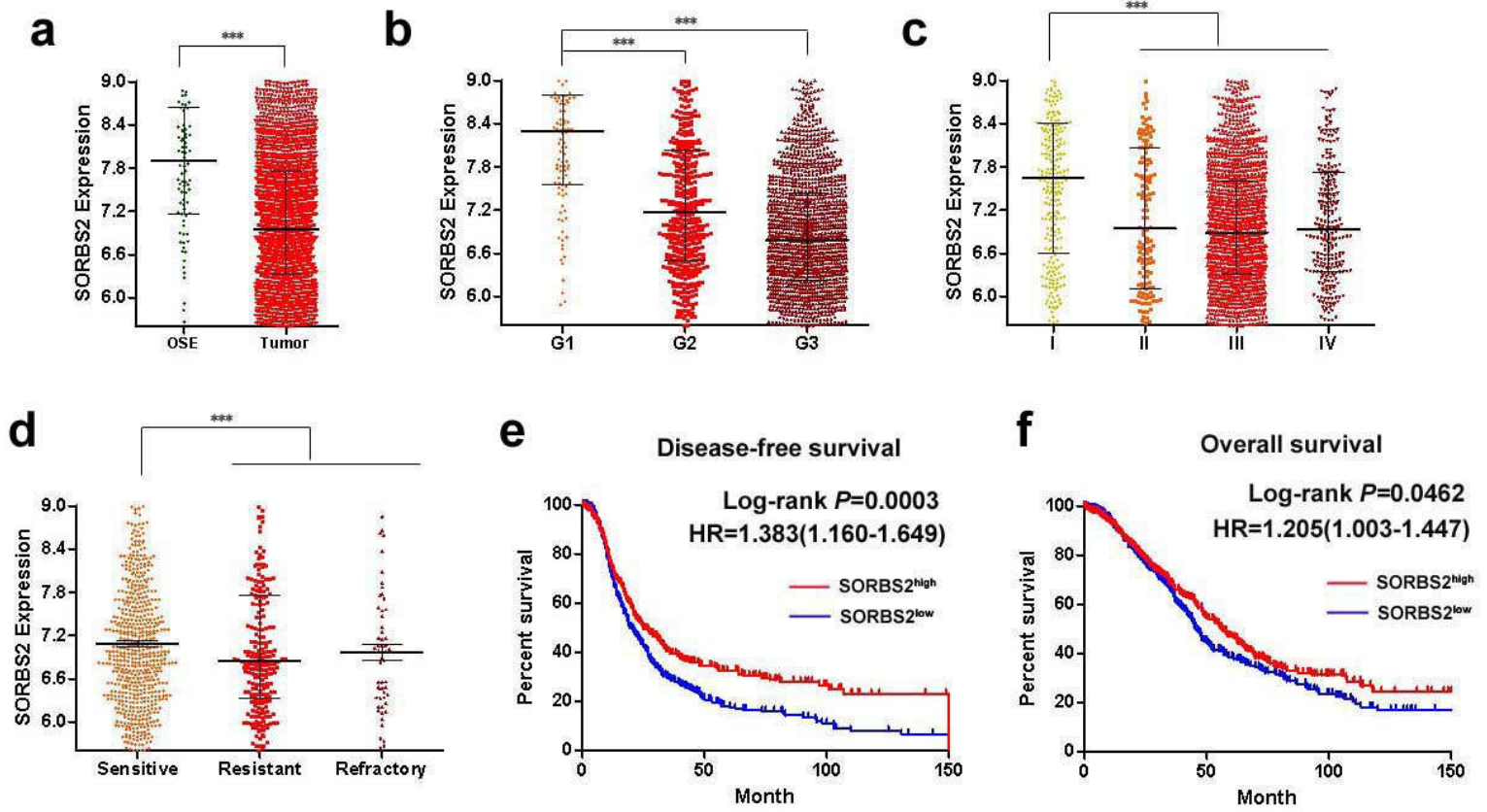


Figure S5

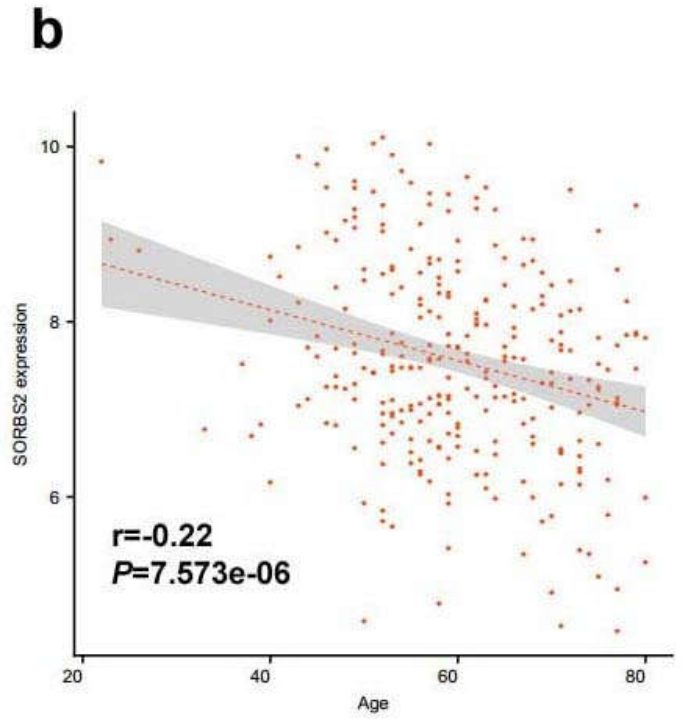
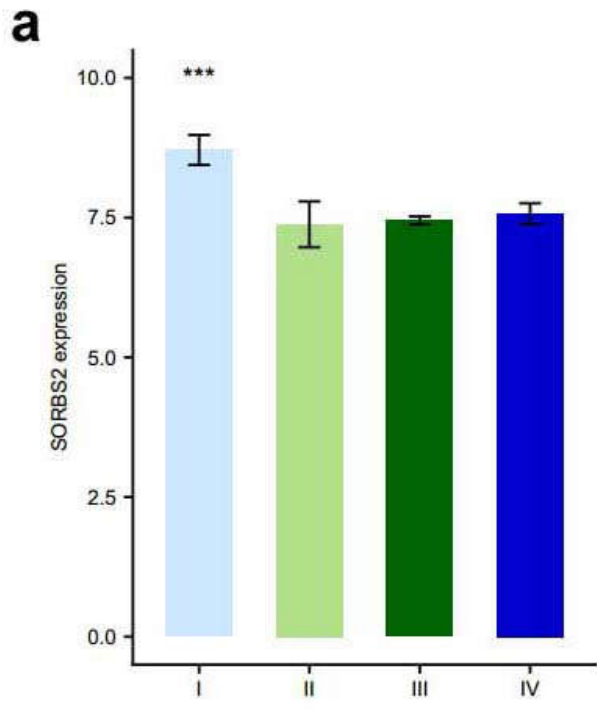


Figure S6

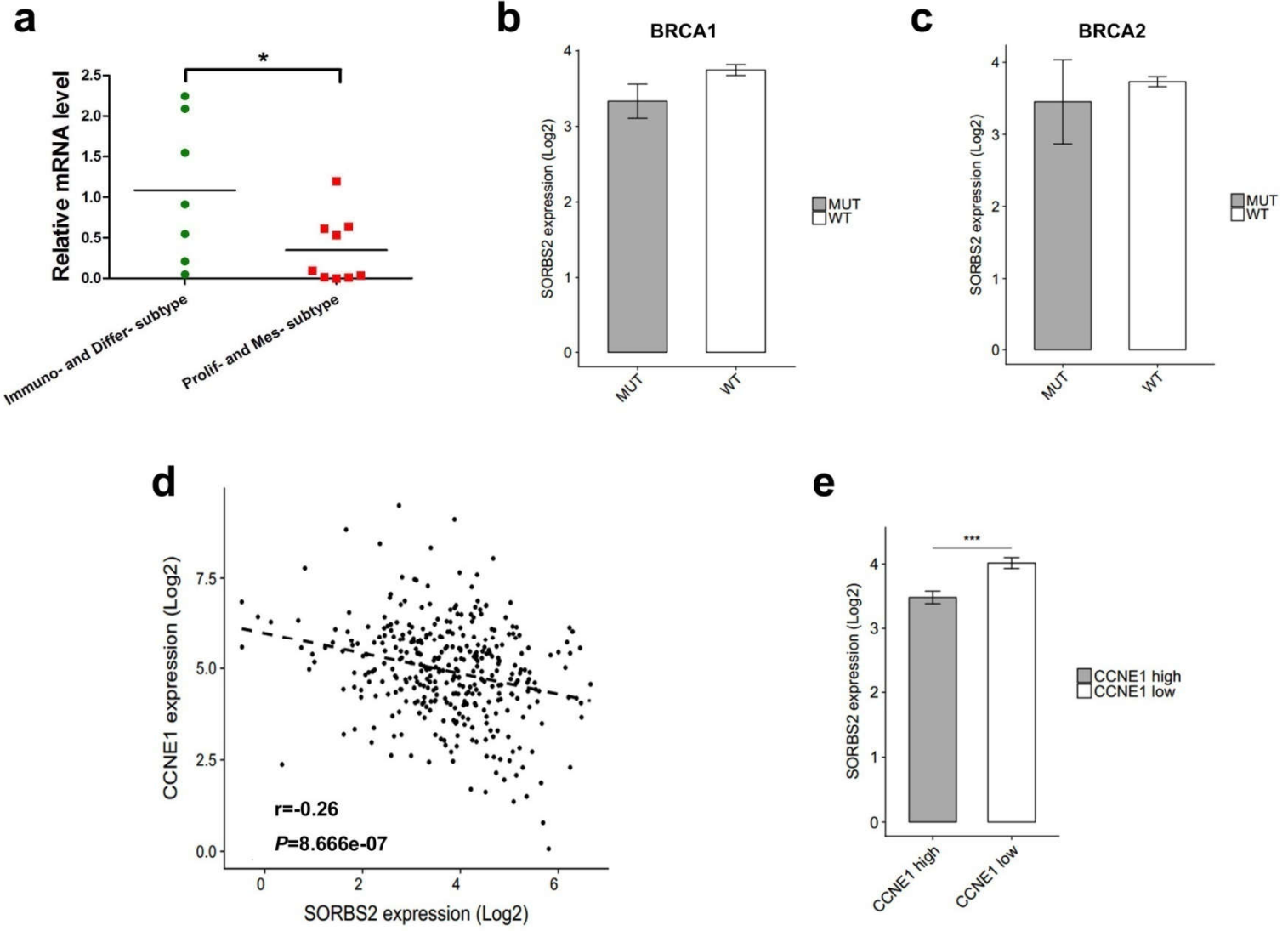


Figure S7

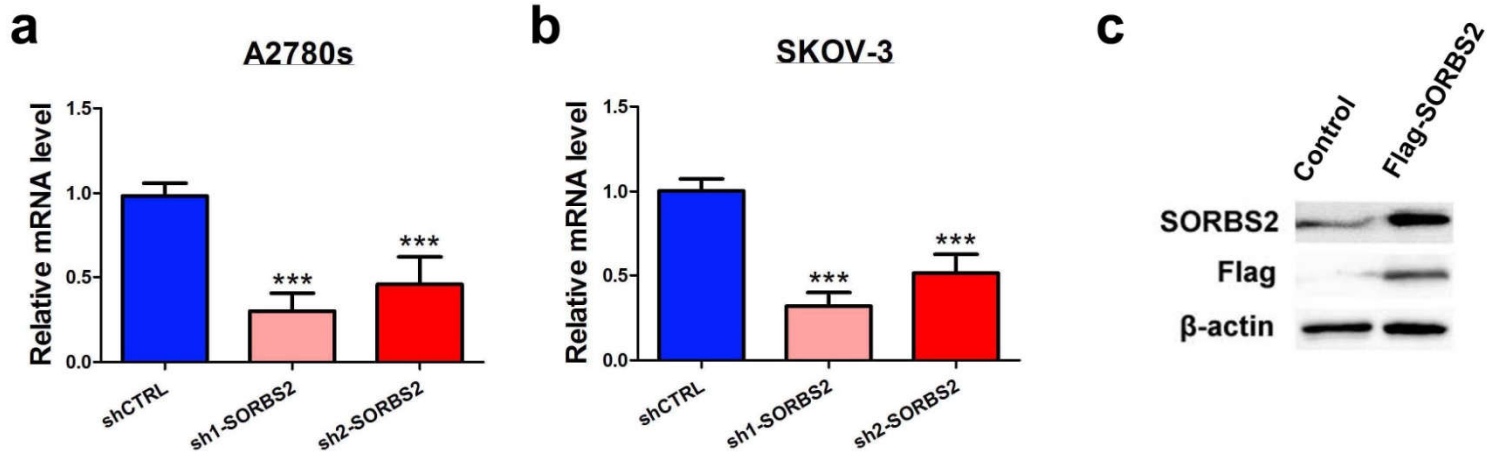


Figure S8

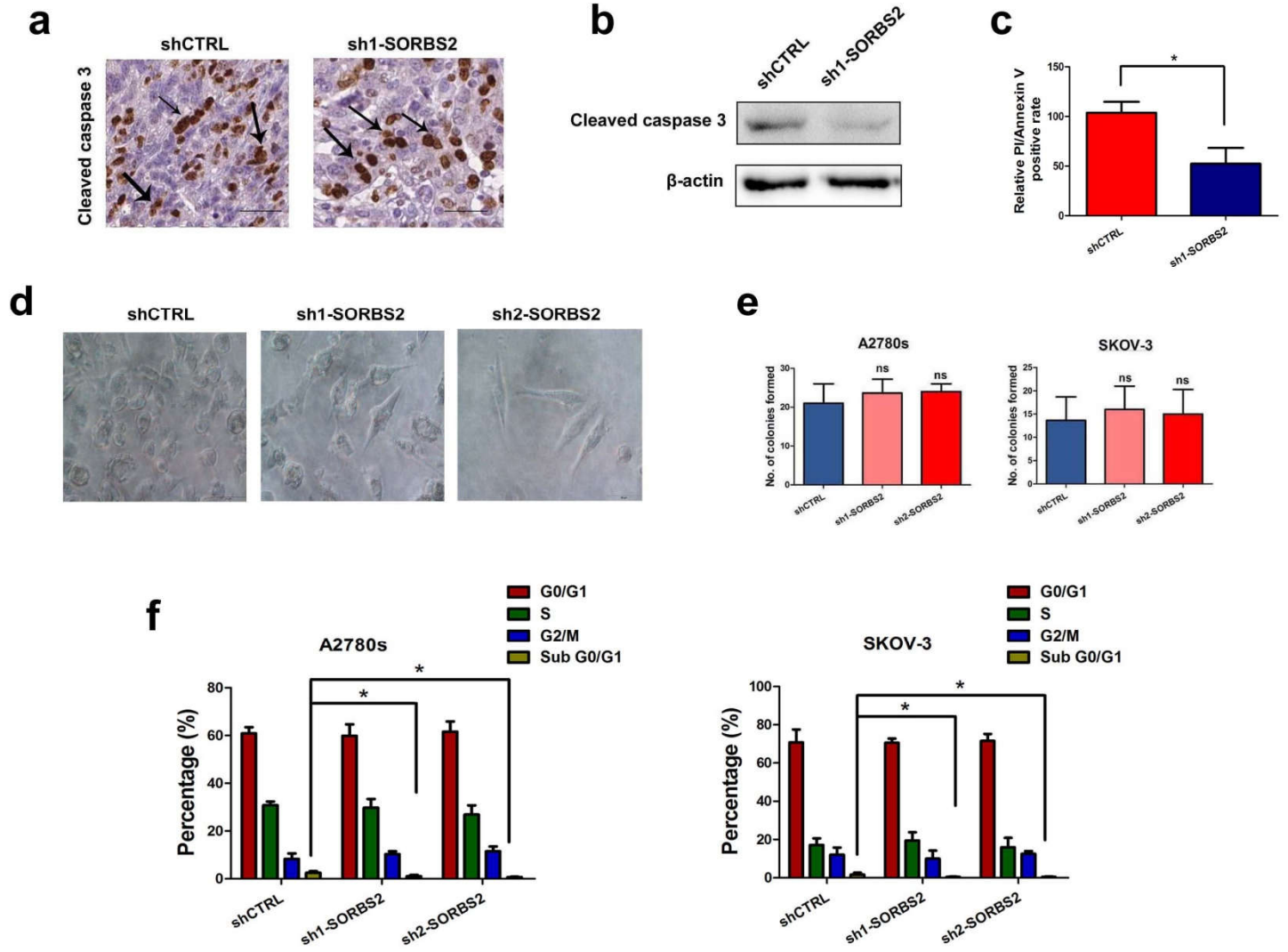


Figure S9

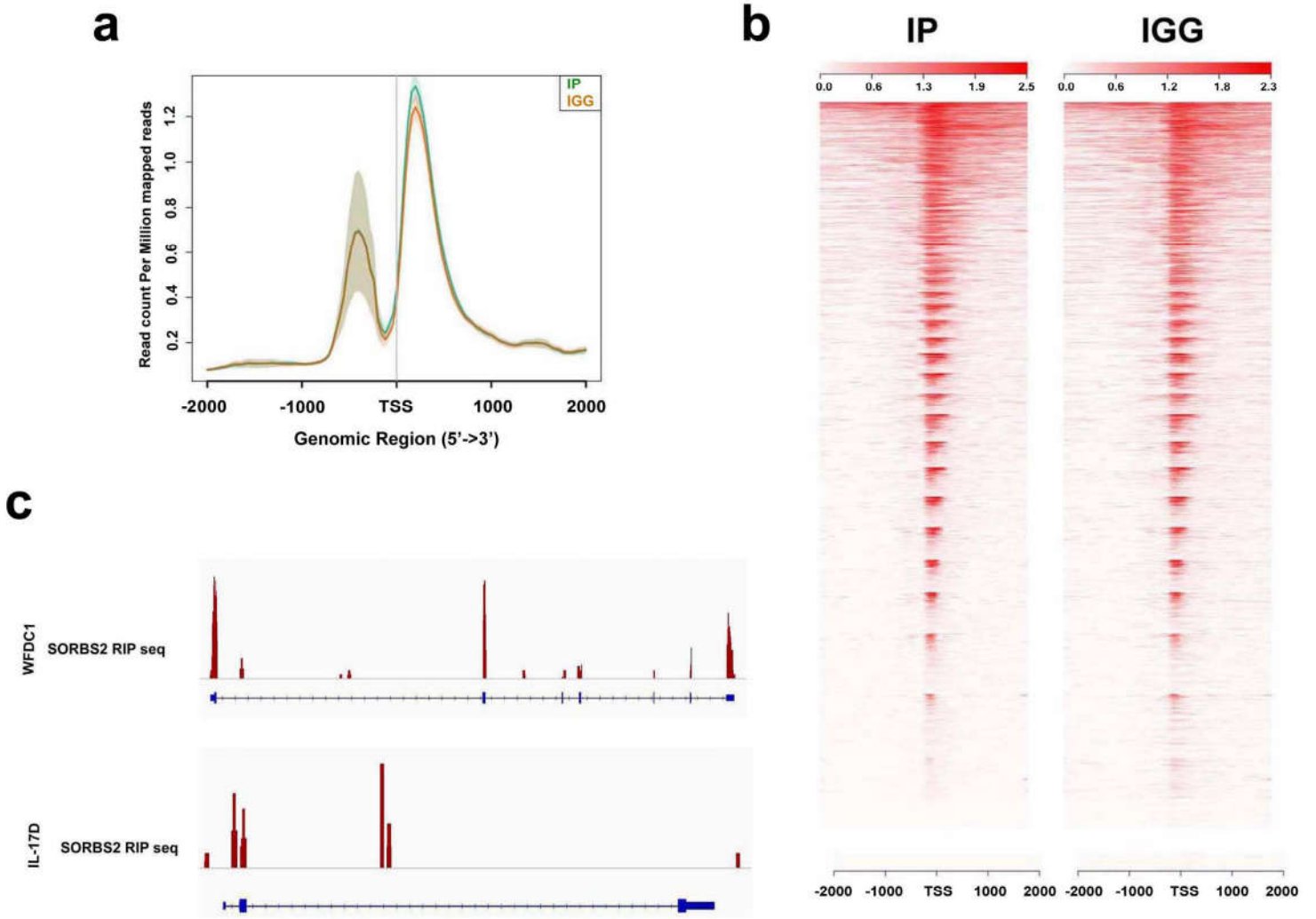


Figure S10

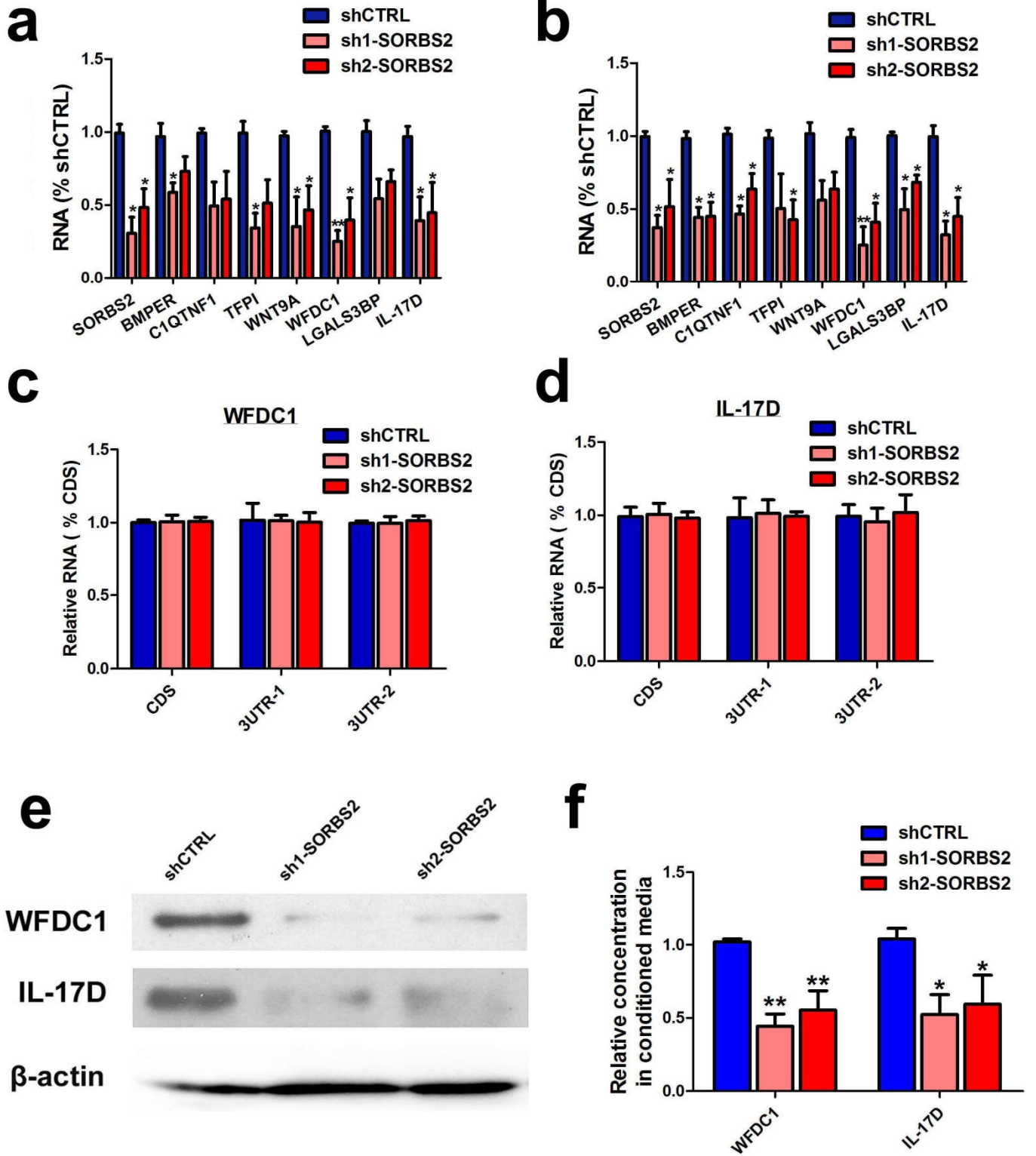


Figure S11

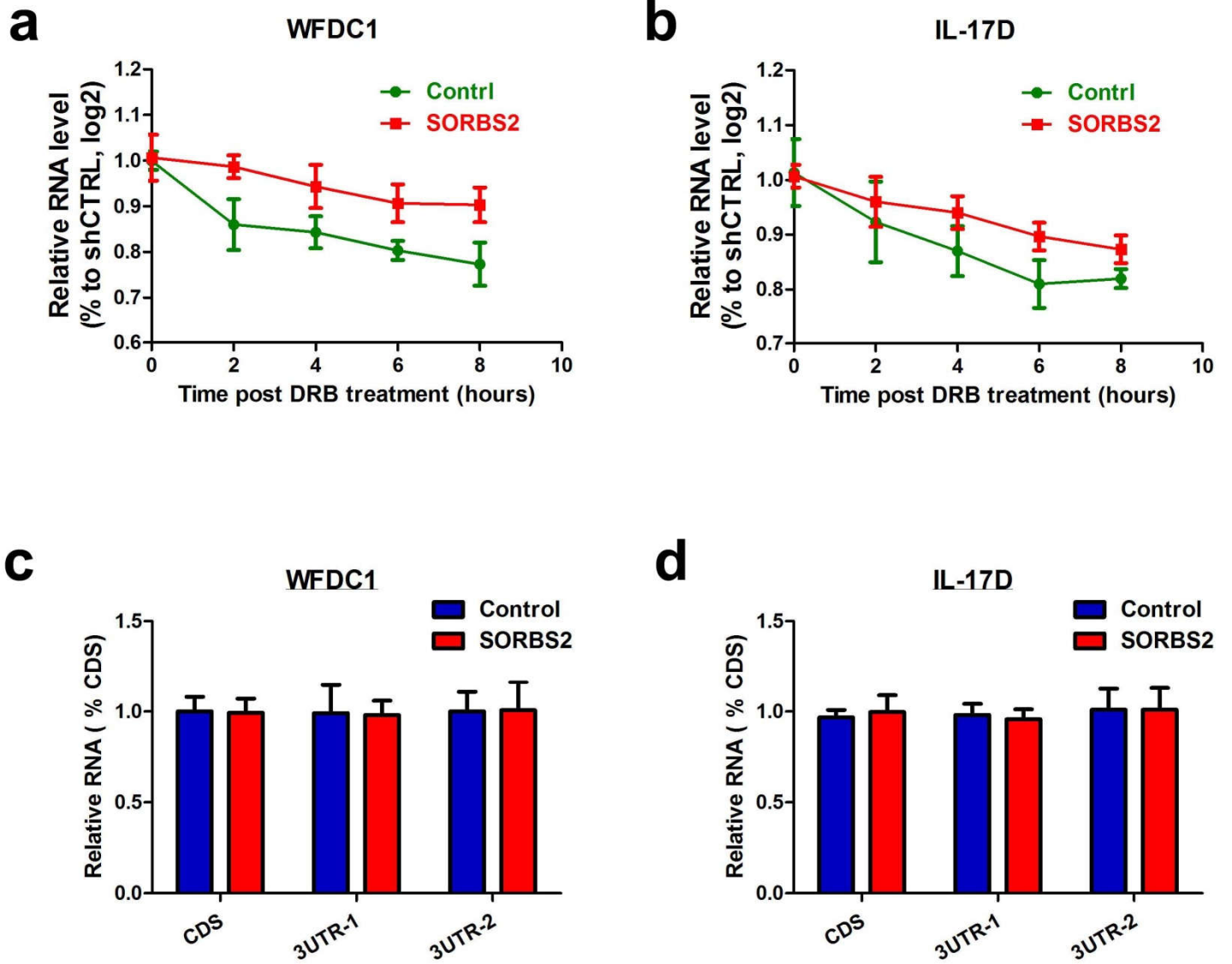


Figure S12

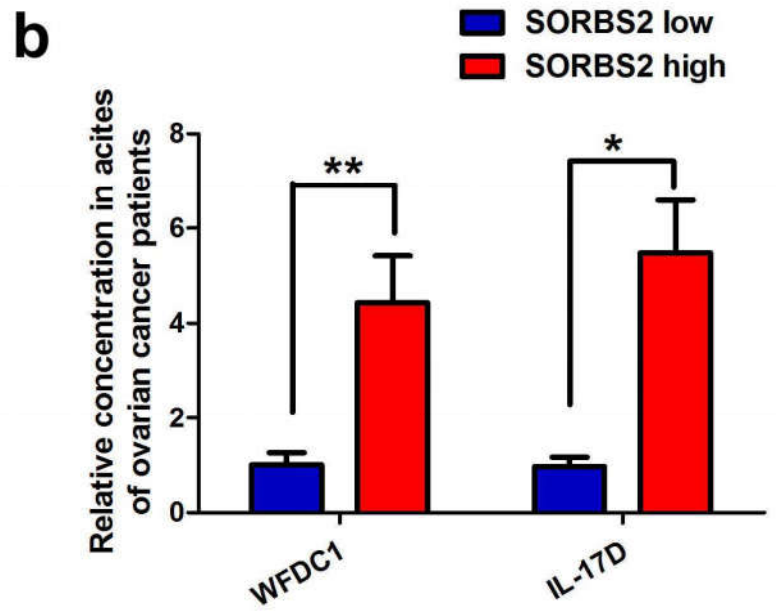
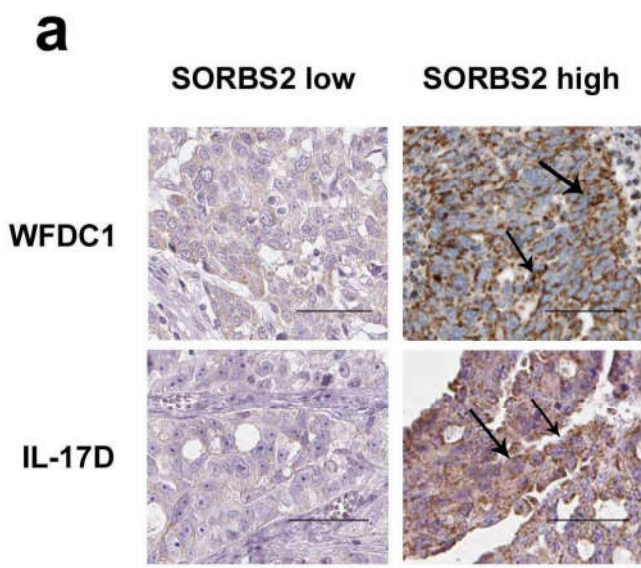
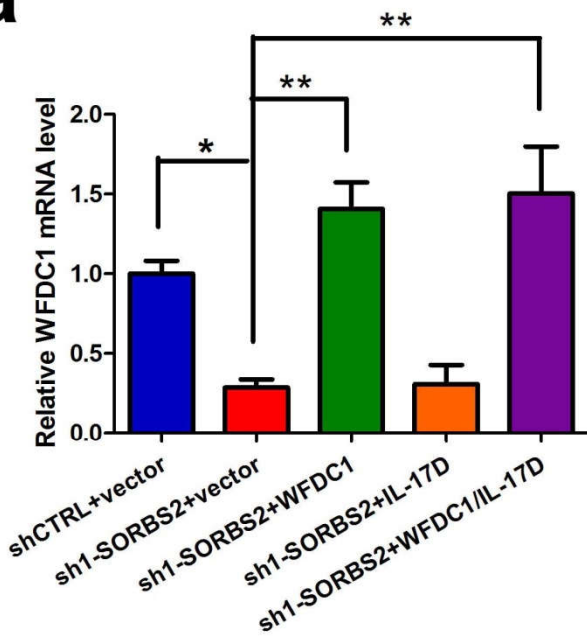
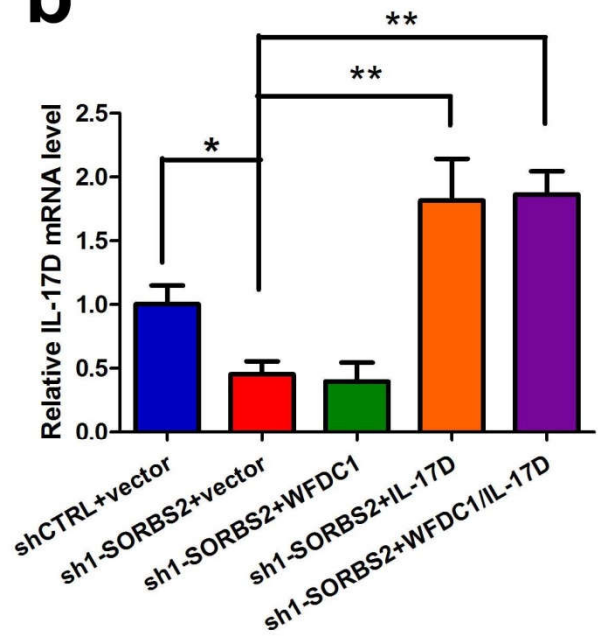


Figure S13

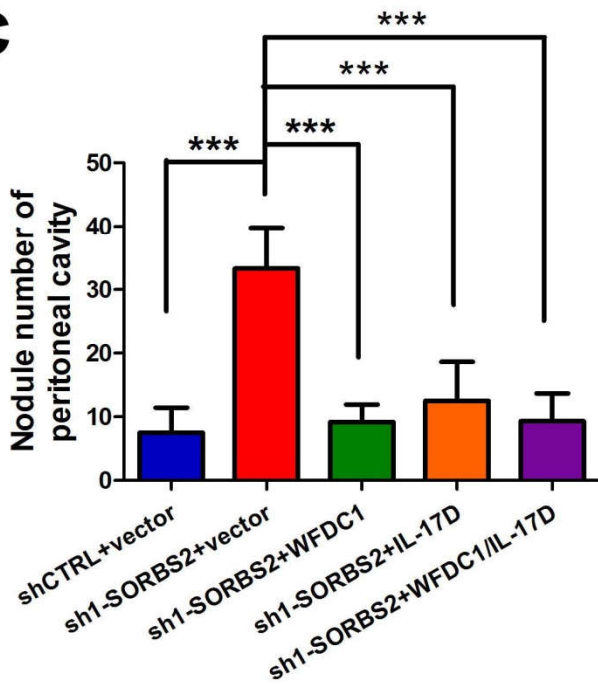
**a**



**b**



**c**



**d**

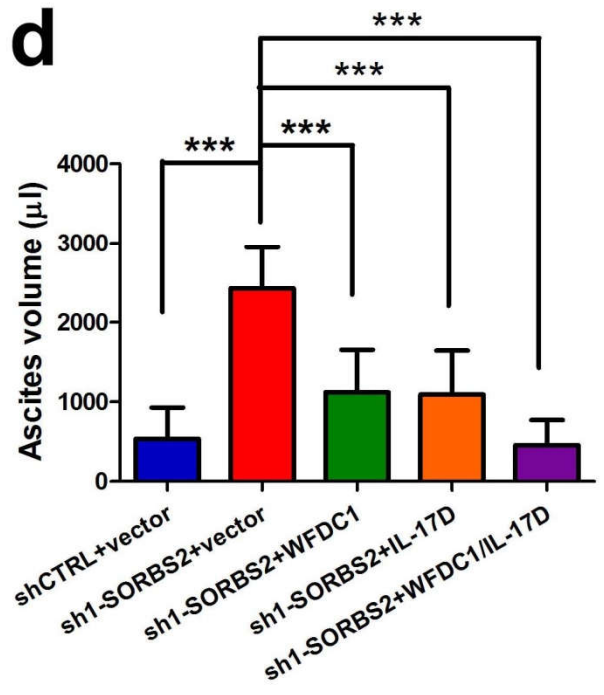
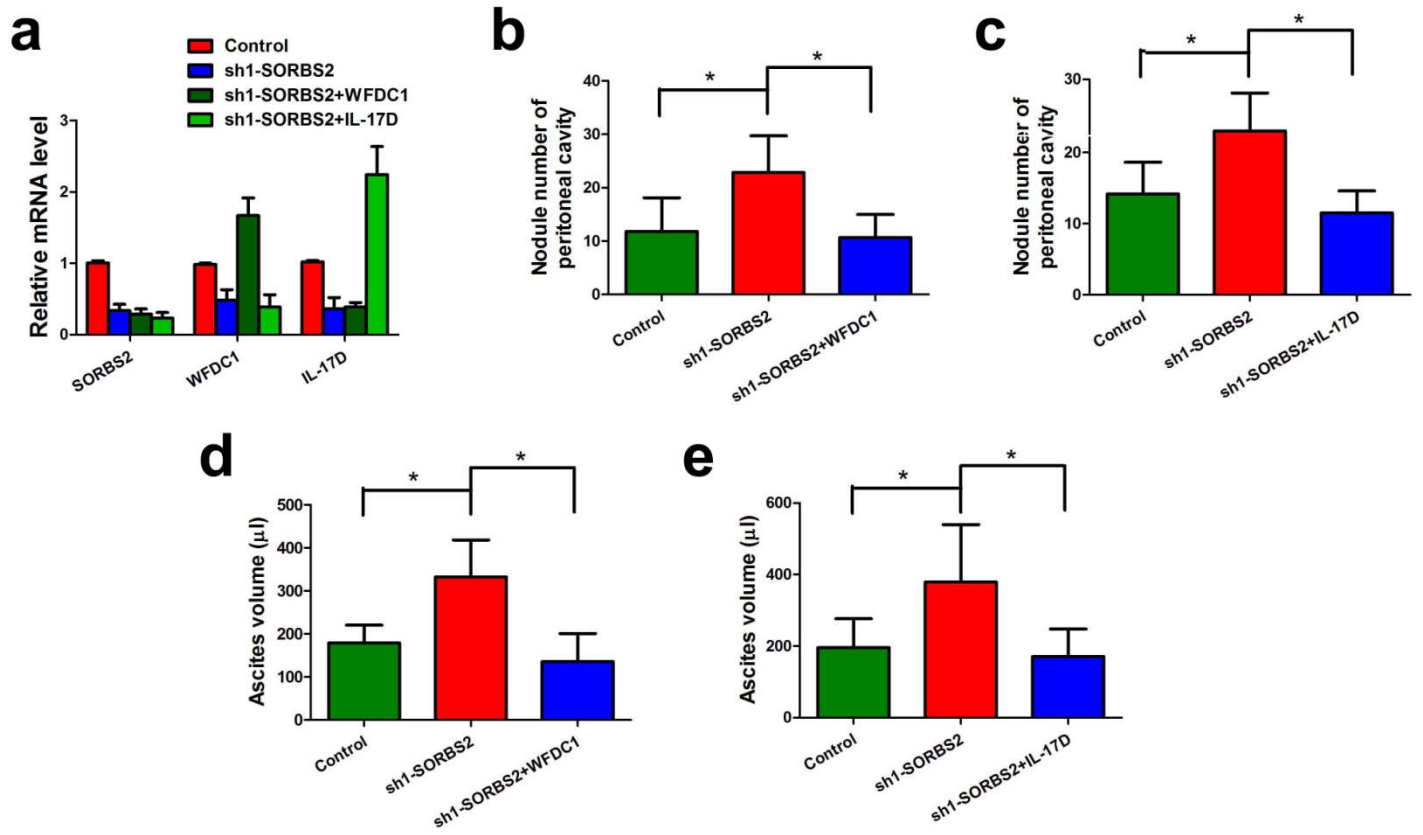


Figure S14



## Supplementary Figure Legends

**Supplementary Figure 1.** Kaplan Meir analysis of the expression of BTF3, CIRBP and MEX3D and clinical outcome of ovarian cancer in AOCS dataset.

### **Supplementary Figure 2.**

**a.** SORBS2 expression in normal ovarian tissues, borderline ovarian tumor tissues and ovarian cancer tissues of datasets in Oncomine database. **b.** SORBS2 expression in different clinical stages of ovarian cancer datasets in Oncomine database. **c.** Immunohistochemistry analysis of SORBS2 expression in normal ovarian tissues and ovarian cancer tissues. **d.** Kaplan Meir analysis of SORBS2 expression and clinical outcome of ovarian cancer in West China Ovarian Cancer cohort.

### **Supplementary Figure 3. SORBS2 suppresses ovarian cancer aggressiveness in clinical samples.**

The expression of BTF3, CIRBP, and MEX3D in primary and metastatic ovarian cancer tissues of datasets in Oncomine database.

### **Supplementary Figure 4. CSIOVDB analysis of SORBS2 expression in ovarian cancer.**

**a.** SORBS2 expression in normal ovary surface epithelium(OSE) and ovarian tumors in CSIOVDB database. **b.** SORBS2 expression in specimens of ovarian cancer with different differentiation grades. **c.** SORBS2 expression in specimens of ovarian cancer with different FIGO stages. **d.** SORBS2 expression in specimens of chemotherapy-sensitive, resistant and refractory ovarian cancer. **e.** Kaplan–Meier analysis of ovarian cancer patients in CSIOVDB database for the correlation between SORBS2 and disease free survival. **f.** Kaplan–Meier analysis of ovarian cancer patients in CSIOVDB database for the correlation between SORBS2 and overall survival. Data are shown as mean  $\pm$ SEM. \*,  $P < 0.05$ ; \*\*,  $P < 0.01$ ; \*\*\*,  $P < 0.001$ .

**Supplementary Figure 5. The correlation of SORBS2 expression with disease stage and age in Tothill dataset.** **a.** The expression of SORBS2 expression in stage I-IV ovarian cancer patients. **b.** Correlation data for SORBS2 versus age in Tothill dataset. The statistical significance of correlations was determined using Pearson's

correlation coefficient. Data are shown as mean  $\pm$ SEM. \*,  $P < 0.05$ ; \*\*,  $P < 0.01$ ; \*\*\*,  $P < 0.001$ .

**Supplementary Figure 6. The expression of SORBS2 in different subtypes of ovarian cancer.** **a.** Expression of SORBS2 in different molecular subtypes of ovarian cancer cell lines. **b.** Expression of SORBS2 in BRCA1 mutant(MUT) and BRCA1 wild type(WT) ovarian cancer tissues in TCGA dataset. **c.** Expression of SORBS2 in BRCA2 mutant(MUT) and BRCA2 wild type(WT) ovarian cancer tissues in TCGA dataset. **d.** Correlation data for SORBS2 versus CCNE1 expression in TCGA dataset. The statistical significance of correlations was determined using Pearson's correlation coefficient. **e.** Expression of SORBS2 in CCNE1 low and CCNE1 high ovarian cancer tissues in TCGA dataset. Data are shown as mean  $\pm$ SEM. \*,  $P < 0.05$ ; \*\*,  $P < 0.01$ ; \*\*\*,  $P < 0.001$ .

**Supplementary Figure 7.**

**a.** mRNA levels of SORBS2 in SORBS2-knock down and control A2780s ovarian cancer cells. **b.** mRNA levels of SORBS2 in SORBS2-knock down and control SKOV-3 ovarian cancer cells. **c.** Protein levels of SORBS2 and Flag in A2780s ovarian cancer cells stably transfected with Flag-SORBS2 plasmid and control. Data are shown as mean  $\pm$ SEM. \*,  $P < 0.05$ ; \*\*,  $P < 0.01$ ; \*\*\*,  $P < 0.001$ .

**Supplementary Figure 8. The impact of SORBS2 depletion on cellular proliferation, apoptosis, cellular morphology and cell cycle *in vitro*.** **a.** Immunohistochemistry analysis of Ki-67 in the tumor tissues of A2780s ovarian cancer cells expressing one of the two independent shRNAs targeting SORBS2 or a control shRNA. **b.** Protein level of cleaved caspase 3 in the lysed tumor tissues of A2780s ovarian cancer cells expressing one of the two independent shRNAs targeting SORBS2 or a control shRNA. **c.** The relative percentage of PI/Annexin V positive cells in the lysed tumor tissues of A2780s ovarian cancer cells expressing one of the two independent shRNAs targeting SORBS2 or a control shRNA. **d.** The representative microscopic photographs of SORBS2-knock down and control A2780s ovarian cancer cells. **e.** Cell proliferation of A2780s and SKOV-3 cells expressing shRNAs targeting SORBS2 or a control shRNA was assessed by colony formation assay. **f.** The percentage of different phases of cell cycles in SORBS2-knock down

and control A2780s and SKOV-3 ovarian cancer cells. Data are shown as mean  $\pm$ SEM. \*,  $P < 0.05$ ; \*\*,  $P < 0.01$ ; \*\*\*,  $P < 0.001$ .

### **Supplementary Figure 9.**

**a.** Transcripts bound by SORBS2 identified by RIP sequencing. IgG was used as negative control. **b.** Heatmap analysis showing RIP sequencing data for SORBS2 and IgG control at a 20-kb region centered over TSS. **c.** SORBS2 RIP-seq read density mapped onto the 3' UTRs of *WFDC1* and *IL-17D*.

### **Supplementary Figure 10.**

**a.** qRT-PCR of candidate SORBS2 target transcripts in A2780s shSORBS2 and shCTRL cells at steady-state. HPRT1 was used as an endogenous control. **b.** qRT-PCR of candidate SORBS2 target transcripts in SKOV-3 shSORBS2 and shCTRL cells at steady-state. HPRT1 was used as an endogenous control. **c.** qRT-PCR for increasingly distal regions of the *WFDC1* transcript 3'UTRs relative to the level of the CDS of each of the genes in A2780s shCTRL and shSORBS2 cells. **d.** qRT-PCR for increasingly distal regions of the *IL-17D* transcript 3'UTRs relative to the level of the CDS of each of the genes in A2780s shCTRL and shSORBS2 cells. **e.** Western blots showing levels of WFDC1 and IL-17D proteins in A2780s shCTRL and shSORBS2 whole cell lysate. Biological triplicates are shown.  $\beta$ -actin was used as a loading control. **f.** Relative concentration of WFDC1 and IL-17D in the conditioned media of A2780s shCTRL and shSORBS2 cells. Data are shown as mean  $\pm$ SEM. \*,  $P < 0.05$ ; \*\*,  $P < 0.01$ ; \*\*\*,  $P < 0.001$ .

**Supplementary Figure 11. The impact of enhanced SORBS2 expression in the transcript stability and 3' UTR lengths of *WFDC1* and *IL-17D*.** **a.** qRT-PCR of relative WFDC1 mRNA level in SORBS2-overexpressing and control A2780s cells at the times indicated after treatment of cells with DRB. **b.** qRT-PCR of relative IL-17D mRNA level in SORBS2-overexpressing and control A2780s cells at the times indicated after treatment of cells with DRB. **c.** qRT-PCR for increasingly distal regions of the *WFDC1* transcript 3'UTRs relative to the level of the CDS of each of the genes in SORBS2-overexpressing and control A2780s cells. **d.** qRT-PCR for increasingly distal regions of the *IL-17D* transcript 3'UTRs relative to the level of the CDS of each of the genes in SORBS2-overexpressing and control A2780s cells. Data

are shown as mean  $\pm$ SEM. \*,  $P < 0.05$ ; \*\*,  $P < 0.01$ ; \*\*\*,  $P < 0.001$ .

### **Supplementary Figure 12.**

**a.** Immunohistochemistry analysis of WFDC1 and IL-17D expression in SORBS2-low and SORBS2-high primary tissues of ovarian cancer. **b.** The relative concentration of WFDC1 and IL-17D in the ascites of ovarian cancer patients in low and high SORBS2 tissues. Data are shown as mean  $\pm$ SEM. \*,  $P < 0.05$ ; \*\*,  $P < 0.01$ ; \*\*\*,  $P < 0.001$ .

### **Supplementary Figure 13.**

**a.** The relative mRNA levels of WFDC1 in A2780s cells stably expressing shCTRL+vector, sh1-SORBS2+vector, sh1-SORBS2+WFDC1, sh1-SORBS2+IL-17D, and sh1-SORBS2+WFDC1/IL-17D. **b.** The relative mRNA levels of IL-17D in A2780s cells stably expressing shCTRL+vector, sh1-SORBS2+vector, sh1-SORBS2+WFDC1, sh1-SORBS2+IL-17D, and sh1-SORBS2+WFDC1/IL-17D. **c.** Box plot of number of metastatic nodules of tumors in the abdominal cavities of mice inoculated with A2780s cells stably expressing shCTRL+vector, sh1-SORBS2+vector, sh1-SORBS2+WFDC1, sh1-SORBS2+IL-17D, and sh1-SORBS2+WFDC1/IL-17D. **d.** Box plot of number of metastatic nodules of tumors in the abdominal cavities of mice inoculated with A2780s cells stably expressing shCTRL+vector, sh1-SORBS2+vector, sh1-SORBS2+WFDC1, sh1-SORBS2+IL-17D, and sh1-SORBS2+WFDC1/IL-17D. Data are shown as mean  $\pm$ SEM. \*,  $P < 0.05$ ; \*\*,  $P < 0.01$ ; \*\*\*,  $P < 0.001$ .

### **Supplementary Figure 14.**

**a.** The transfection efficacy was evaluated by measuring the mRNA levels of each gene in each group. **b.** The number of metastatic nodules of C57BL/6 mice model intrabursally inoculated with control ID-8 cells, SORBS2-knockdown ID-8 cells and WFDC1 overexpressing SORBS2-knockdown ID-8 cells at sacrifice. n=6 in each group. **c.** The number of metastatic nodules of C57BL/6 mice model intrabursally inoculated with control ID-8 cells, SORBS2-knockdown ID-8 cells and IL-17D overexpressing SORBS2-knockdown ID-8 cells at sacrifice. n=6 in each group. **d.** The ascites volume of C57BL/6 mice model intrabursally inoculated with control ID-8 cells, SORBS2-knockdown ID-8 cells and WFDC1 overexpressing

SORBS2-knockdown ID-8 cells at sacrifice. n=6 in each group. **e.** The ascites volume of C57BL/6 mice model intrabursally inoculated with control ID-8 cells, SORBS2-knockdown ID-8 cells and IL-17D overexpressing SORBS2-knockdown ID-8 cells at sacrifice. n=6 in each group. Data are shown as mean  $\pm$ SEM. \*,  $P < 0.05$ ; \*\*,  $P < 0.01$ ; \*\*\*,  $P < 0.001$ .